An Optimum Routine for Surface Modification of Ceramic Supports to Facilitate Deposition of Defect-Free Overlaying Micro and Meso (Nano) Porous Membrane

Ahmadian Namini, Pejman; Babaluo, Ali Akbar *+; Jannatdoust, Elham•;
Peyravi, Majid; Akhfash Adrestani, Masoumeh
Nanostructure Materials Research Center (NMRC), Sahand University of Technology,
P.O. Box 51335-1996 Tabriz, I.R. IRAN

ABSTRACT: *In this work, a simple and effective way to modify the support surface is developed and a nanostructure ceramic support to facilitate deposition of a defect-free overlying micro and meso (nano) porous membrane is obtained. To achieve high performance nanocomposite membranes, average pore size of outer surface of support was reduced by dip-coating in submicron and nano α-alumina slurries. In this respect, the effects of several parameters such as: solid content, dipping time, vacuum pressure, heating rate and number of coated layers on microstructure of the fabricated layers were investigated. The obtained results showed that the optimum routine for this technique was twice coating of 5wt% submicron slurry without applying vacuum followed by vacuum dip-coating of 5wt% submicron and 1wt% nano alumina slurry. Pore size of the unmodified membrane support was calculated using permeance data and the obtained result was 540 nm. After twice modification with submicron alumina slurry without vacuum, average pore size of surface decreases significantly. More surface modification by vacuum dip-coating of alumina submicron and nano particles slurries results in decreasing of average pore size of intermediate layers to nanometric scale (<100 nm), respectively. The obtained results are confirmed by mercury porosimetry measurements.*

KEY WORDS: *Nanostructure membrane support, Ceramic, Dip-coating, Gas permeation, Pore size.*

INTRODUCTION

Membrane processes are being used more and more in many fields such as filtration, distillation, separation or extraction [1]. The use of membrane technology to replace a separation or purification step in an industrial process may reduce the overall consumption of energy [2]. Until recently, the industrial membranes were manufactured from polymeric materials. However, the major drawback is that the thermo mechanical and chemical stability of the conventional polymeric membranes is limited with respect to high temperature and corrosive media like strong acids and organic solvents. Therefore, many researches to date focus on ceramic membranes [1, 3-8].

Commercialization of such devices requires meeting of often incompatible goals, namely high permeability, chemical and thermal stability and mechanical strength [9]. Ceramic membranes with high performance parameters such as high permeability and permselectivity can only be obtained in an asymmetric multilayer configuration: a) a high-quality macroporous support system providing mechanical strength to the system, b) mesoporous intermediate layers whose roles are to reduce any inherent defects of the support and to prevent the infiltration of top layer material into the pores of support and c) a microporous separation top layer which only allows certain material to transport through the membrane [3,7,10-12].

It has been known that the quality of the underlying support determines, to a high degree, the properties and quality of the top selective microporous layer. Coarse or large-pore support surfaces would cause cracking of overlying layers due to stress development on uneven film coatings [13]. Therefore, it is important to develop a simple and effective way to modify the support surface to facilitate deposition of a defect-free overlying microporous layer.

A variety of methods have been proposed for the modification of porous supports, including sputtering, spray or dip coating, slip or solution casting, pulsed laser deposition, and chemical or electrochemical vapor deposition [9,13-16]. Among these, dip-coating with its various advantages such as excellent processibility, uniform surface and high potential to precisely control of pore size and pore structure could be attracted much attention in the scientific community.

Due to our knowledge, there are a few studies that have examined the fabrication of intermediate layers via dip-coating method and investigated the effects of key parameters on the morphology and microstructure of the dip-coated intermediate layers in nanostructure ceramic composite membranes. Moreover, the aspect of porosity of alumina supports modified by dip-coating method has not been discussed yet. Consequently, more researches in this area are needed.

The main objective of the present work is to develop a simple and effective way to modify the support surface and to attain a nanostructure ceramic support to facilitate deposition of a defect-free overlying micro and meso (nano) porous membrane. In this respect, the effects of several key parameters on the prepared layers microstructure and morphology were investigated and an optimum routine

for this technique was presented. Also, results of single gas permeation test were used to determine average pore size of the fabricated intermediate layers. The obtained results were verified by mercury porosimetry.

EXPERIMENTAL SECTION

Tubular alumina supports (15 mm diameter, 3 mm thickness and 75 mm length) were prepared by gel-casting as a novel forming method [17]. Nanostructure support intermediate layer composed of two concentric layers with a decreasing pore size which were made-up with in-house synthesized submicron and nano alumina powders (submicron powder: 240 nm [18] and nano powder: 50 nm [19]).

Dip-coating method was utilized for preparing the interlayers. In this respect, the effects of several parameters such as solid content, dipping time, vacuum pressure, heating rate and number of coated layers on the prepared layers microstructure and morphology were investigated.

Intermediate layers fabrication

Deposition of α-Al_2O_3 intermediate layer was performed by a colloidal processing. Stable submicron alumina suspension has been prepared using 5 wt % α-Al_2O_3 (in-house synthesized submicron powder, 240 nm [18]), 0.3 mL (per 100 g of ceramic powder) of polyacrylic acid ammonium salt (Darvan 821-A, R.T. Vanderbilt) and 5 wt % (based on ceramic powder) of polyethylene glycol with molecular weight of 6000 g/mol (PEG6000, Merck Co.) as polymeric binder. Similarly, stable nano alumina suspension has been prepared using 1 wt % α-Al_2O_3 (in-house synthesized nano powder, 50 nm [19]), 0.3 mL (per 100 g of ceramic powder) of polyacrylic acid ammonium salt (Darvan 821-A, R.T. Vanderbilt) and 5 wt % (based on ceramic powder) of polyethylene glycol with molecular weight of 6000 g/mol (PEG6000, Merck Co.).

Intermediate layers were obtained by dipping the support in the prepared suspension and standing for a distinct time and vacuum pressure and then raised up with velocity of 40 mm/min. The system was dried for 24 h at ambient temperature and was sintered vertically at 1350 $^\circ$C for 2 h. The procedure was gone over several times with adjusted parameters to attain a surface with desirable characteristics.

Characterization

The optical microscopy images of surface of the fabricated layers were taken using Olympus PMG3

digital camera. The surface and cross-sectional microstructure of the multilayer ceramic membrane supports were studied by Scanning Electron Microscopy (SEM, CamScan MV2300 and LEO 440I, UK). Mercury porosimeter (Pascal 440, 1.8-7500nm, Thermo Finnigan Co., Italy) measurements were performed to determine the open porosity, pore size and Pore Size Distribution (PSD) of the fabricated multilayer membrane supports.

Average pore size of the prepared layers was determined from mercury porosimetry data using following equation:

$$\bar{r} = \frac{\int_{r_1}^{r_2} rV(r)dr}{\int_{r_1}^{r_2} V(r)dr} \tag{1}$$

where $\bar{r}$ is average pore size of layer, r is pore radius, $V(r)$ is pore volume, and r_1 and r_2 are lower and upper boundaries of pores radius range, respectively.

Permeation studies
Theory

The modified ceramic supports usually have multilayer composite structures, supposing that the surface diffusion of powder is negligible and layers have narrow pore size distribution. It is reasonable that a pore size averaged along the gas diffusion direction is used to designate pore size for each layer prepared in the modification procedure.

The most common methods for determining the pore size of porous ceramic membranes are gas adsorption and mercury porosimetry [20-21]. In these methods, pore size distribution and average pore size of porous membranes are calculated from the adsorption and desorption isotherms measured by commercially available adsorption porosimeters.

In this investigation, a simple gas permeation method was used to examine average pore size of ceramic membrane support. In this method, an argon flow at a given flow rate (Q) was passed through a porous membrane support sample. After reaching steady-state, an upstream pressure (P_h) and a downstream pressure (P_l) were measured by pressure meters. Gas permeance was calculated using the following definition:

$$(F/L) = Q / \left[S_{t_0} (P_h - P_l) \right] \tag{2}$$

Where L is thickness and S_{t_0} is total permeation area of tubular porous support. Permeance data at different average pressures $\left[P_{av} = (P_h + P_l)/2 \right]$ were measured and the obtained results were plotted as (F/L) versus P_{av} and regressed with the following linear equation:

$$(F/L) = \alpha + \beta P_{av} \tag{3}$$

Experimental value of (β/α) for the membrane support are used to examine average pore size ($\bar{r}$) by the following equation [22]:

$$\bar{r} = \left[8.47 \mu (R_g T/M)^{1/2} \right] (\beta/\alpha) \tag{4}$$

where T is absolute temperature, M is molecular weight, μ is viscosity of permeating gas and R_g is the gas constant.

The above analysis is now extended to composite (multilayer) membrane supports consisting of two layers with different pore structures. For two-layer composite membrane supports consisting of unmodified support and top-layer, as shown in Fig. 1, it could be assumed that the whole thin top-layer have a same pore structure and is much thinner than support.

For two-layer system, applying Eq. (3) to support and top-layer gives the following equations correlating permeation flow to the argon pressure at different locations across the membrane sample:

$$Q = S_{t_0} \left[\alpha_t + 0.5 \beta_t (P_h + P_m) \right] (P_h - P_m) \tag{5}$$

$$Q = S_{t_0} \left[\alpha_s + 0.5 \beta_s (P_m + P_l) \right] (P_m - P_l) \tag{6}$$

where subscripts s, t and m denote support, top-layer and interface of layers, respectively. P_m is pressure at interface of two layers and can be found by solving Eq. (6). α_t and β_t can be obtained by rearranging Eq. (5):

$$Q / \left[S_{t_0} (P_h - P_m) \right] = \alpha_t + \beta_t \left((P_h + P_m)/2 \right) \tag{7}$$

Permeance for the whole two-layer system could be written as:

$$(F/L)_{av} = Q / S_{t_0} (P_h - P_l) = F(P_h, P_l, \alpha_s, \alpha_t, \beta_s, \beta_t) \tag{8}$$

Eq. (8) could be rearranged to the same linear form as Eq.(3):
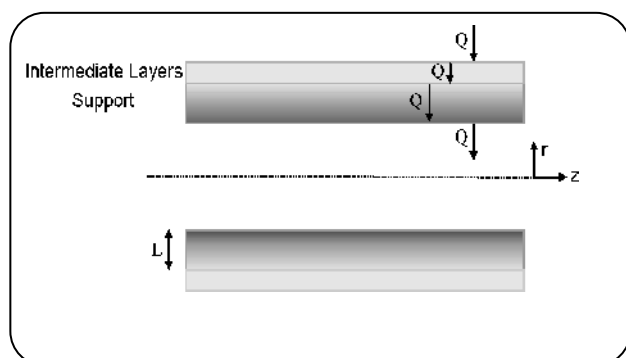
$$(F/L)_{av} = \alpha_{av} + \beta_{av} P_{av} \tag{9}$$

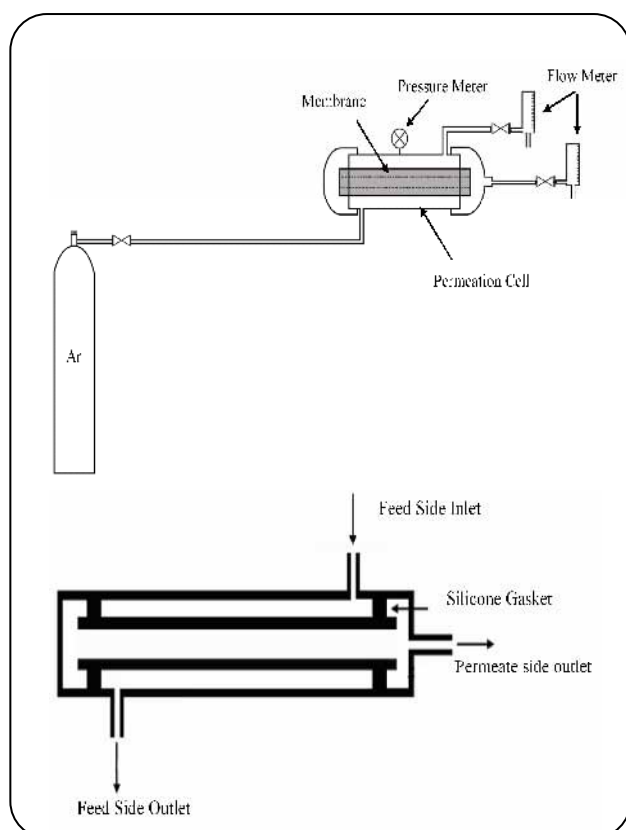**Fig. 1: Schematic of tubular multilayer ceramic support.**

Fig. 2: Schematic of tubular permeator.

where α_{av} and β_{av} are average permeability coefficients for the whole two-layer composite support. The calculated α_{av} and β_{av} from whole gas permeation data were considered as α_s and β_s of two-layer system as support for the next top-layer, respectively.

Gas permeation experiments

Single gas permeation measurement was carried out in ambient conditions to evaluate quality and determine

average pore size of ceramic composite membrane supports. Measurements of H_2 and N_2 permeation were made at pressure differences up to 6 bar. Permeance was measured using the stainless steel permeator shown schematically in Fig. 2. Both annular ends between the membrane support tube and the permeator wall were sealed with moulded RTV silicone gasket rings. Feed gas flows along outside of the membrane support and permeated gas flow rate were measured on inner side of the membrane support tube at pressure 1 bar. Pressure differences across the membrane support were obtained by varying pressure on the upstream side and keeping the downstream pressure constant at 1 bar. Pressure in shell side of the membrane module was monitored via a pressure gauge.

RESULT AND DISCUSSION

Membrane intermediate layers microstructure

The effects of several parameters such as solid content, dipping time, vacuum pressure, heating rate and number of coated layers on microstructure of the fabricated layers were investigated. Due to the presence of polymeric binder and dispersant, the heating rate has to be carefully controlled to avoid build up of surface cracks. Heating rates of 4, 2, 1 and 0.5 °C/min were examined for debinding stage up to 850 °C. The heating stage followed by increasing of temperature at a rate of 5 °C/min up to 1350 °C and the articles were maintained at this temperature for 2 hours and cooled slowly to ambient temperature. Fig. 3 shows the SEM images of the sintered articles surfaces with different heating rates. As can be seen, decreasing of the heating rate to 1 °C/min results in a significant decrease in the cracks size and more uniform surface. Further decreasing of heating rate to 0.5 °C/min, has no considerable effect on surface qualify of the intermediate layers. This trend can be due to this fact that debinding rate of polymeric materials increases by increasing heating rate, resulting in a significant increment of surface cracks build up.

Applying 0.02-0.03 bar vacuum in the fabrication of intermediate layers results in constitution of more even surfaces (see Fig. 4). On the other hand, using vacuum at the first coating step causes undesired penetration of submicron particles in pores of the unmodified support systems, so that the more vacuum pressure, the more powder penetration (see Fig. 5). This trend could reduce the permeation of support dramatically. Thus, the first dip-coating step was done without applying vacuum.
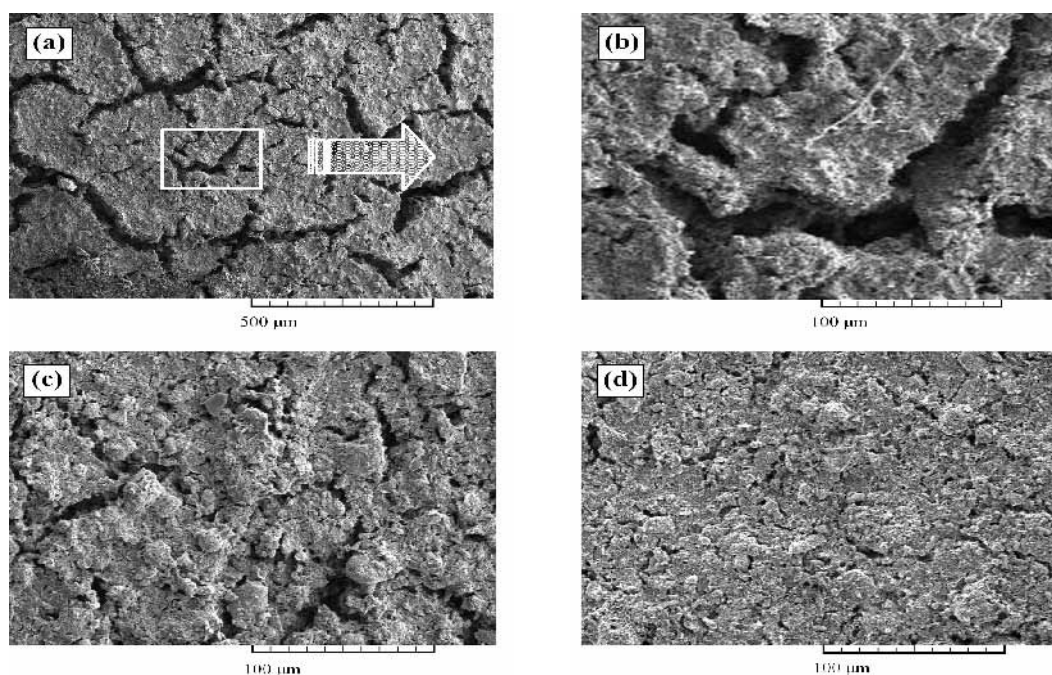
Fig. 3: SEM images of coated layers surfaces with different heating rates of debinding: (a, b) 4 °C/min, (c) 2 °C/min and (d) 1 °C/min.
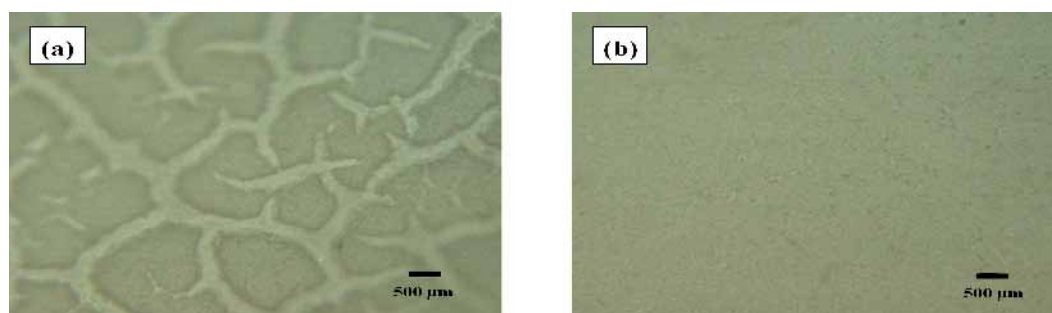

Fig. 4: Optical microscopy images of coated layer surface: (a) without and (b) with applying vacuum.

Fig. 6 shows the effect of number of coating layers (without applying vacuum) on the surface quality. After two dip-coating steps, smoother surface was achieved and cracks size was reduced dramatically. By employing another coating step, no significant change was observed and so two dip-coating steps without applying vacuum were employed and one vacuum dip-coating step was performed subsequently to achieve smoother surface.

Dipping time and solid content have similar effects on the fabricated layer microstructure and quality. By increasing solid content from 5 to 10 and 20 wt %, cracks appear on the layers surface before thermal treatment which is related to high thickness of the coated layers (see Fig. 7). By the same reason, by increasing dipping time, the thickness of layer increases and coated layer is practically fully separated from the support before thermal treatment. Consequently, for the dip-coating process, slurries of 5 wt % ceramic powder were applied. Also, based on our previous work results [17], the dipping times of 30 s and 15 s were employed as maximum allowed time to avoid crack formation (prior to thermal treatment) for coating process without and with applying vacuum, respectively.
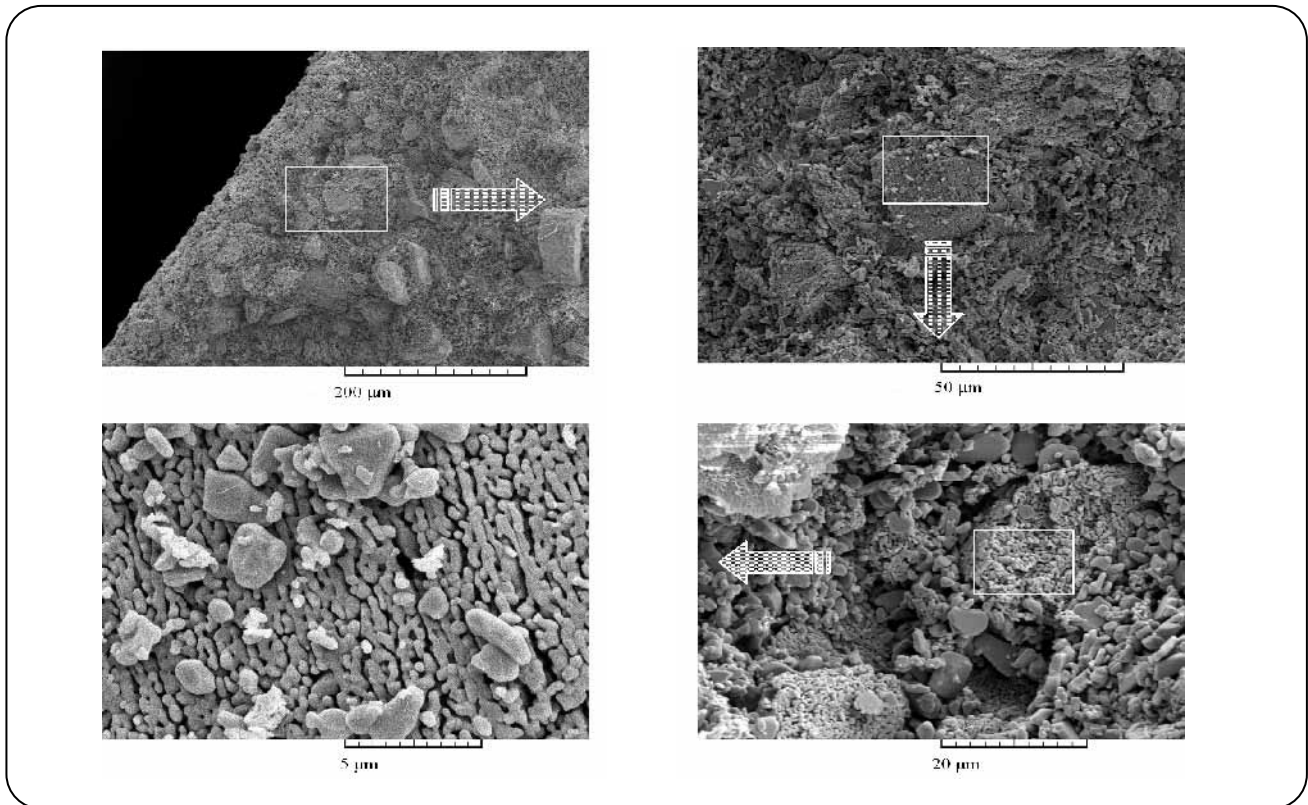
Fig. 5: SEM images of supports cross section prepared with applying 0.02-0.03 bar vacuum at the first coating step.
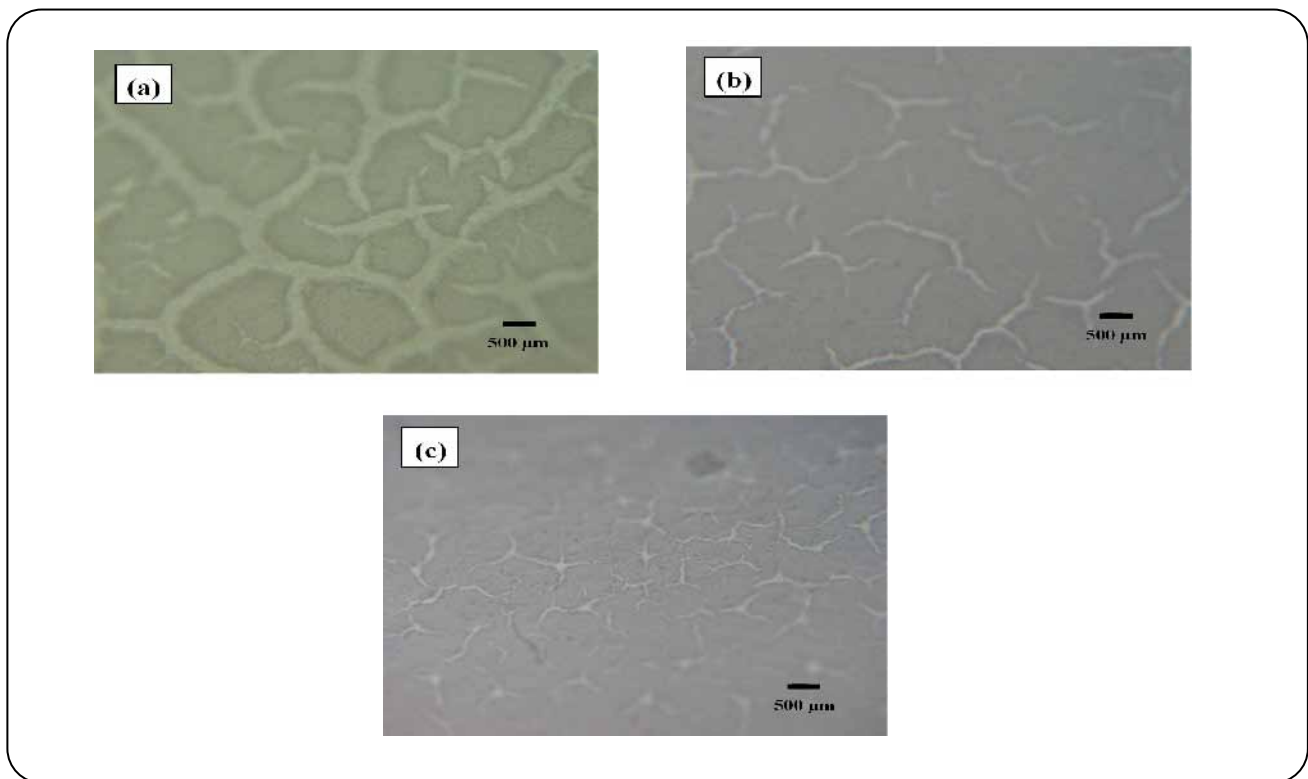

Fig. 6: Optical microscopy images of support surface after (a) 1, (b) 2 and (c) 3 dip-coating steps without applying vacuum.

Table 1: Identifying code for each step of modification procedure.

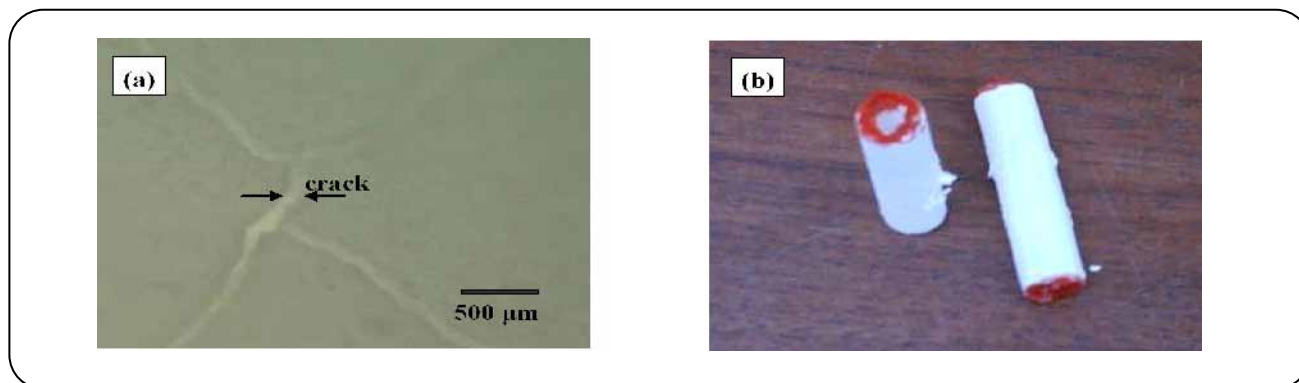| Modification step	Condition	Molecular formula
1	Untreated Support	Sup
2	1 submicron coating without vacuum	Sub_1
3	2 submicron coating without vacuum	Sub_2
4	1 submicron coating with vacuum	Sub_2V
5	1 nano coating with vacuum	Sub_2Vnano

Fig. 7: (a) Optical microscopy image of sample prepared by 10 wt %and (b) image of sample prepared by 20 wt% slurries before thermal treatment.

After multi-coating of submicron slurry, another vacuum dip-coating stage was performed with slurry of 1 wt % nano alumina powder to obtain a nanostructure surface with more desirable performance. For ease in nomination, an identifying code has been assigned to each step in the modification procedure as presented in Table 1.

The SEM images of intermediate layer surface and cross view for various steps of modification procedure are shown in Fig. 8. As can be seen, by applying the mentioned modification procedure, after vacuum coating of submicron powder slurry and afterwards vacuum coating of nano powder slurry, an even surface with reduced pore size was achieved and cracks of surface were disappeared significantly.

Also, the thickness of intermediate layers fabricated after different modification steps were presented in Table 2. As can be seen, by applying the mentioned conditions via dip-coating method the intermediate layers were fabricated successfully over the support and no penetration of intermediate layers in the unmodified support could be observed. With regards of the SEM images, the fabricated nanostructure ceramic supports promote a high performance in membrane separation processes due to its defect-free surface and multilayer structure with no penetration.

Membrane intermediate layers pore size

Mercury porosimetry results for Sup., Sub_2 and Sub_2Vnano samples are shown in Fig. 9 and Fig. 10 (a) and (b), respectively.

By using Eq. (1) for porosimetry data of unmodified support, the calculated average pore size was 540 nm. For Sub_2 and Sub_2Vnano samples, calculations were done using Eq. (2) after omitting the data of unmodified support. Average pore sizes of 143 nm and 89 nm were calculated for Sub_2 and Sub_2Vnano samples, respectively.

As mentioned earlier, average pore size ($\bar{r}$) of each layer were calculated from the permeation data. For the unmodified membrane support, the values of α_s and β_s were calculated from permeation data (permeance) plotted versus average pressure (see Fig.11) and using Eq. (2). Average pore size of the unmodified support ($\bar{r_s}$) was obtained 539.76 nm by applying Eq. (3) (see Table 2).

For the next layers, average pore size value was also calculated from gas permeance results. Fig. 12 shows results of the argon permeance through a multilayer

Table 2: The values of L, α, β and $\bar{r}$ for multilayer ceramic support.

Membrane layer	Thickness (L) μm	α $10^{-8}\,mol\,/(s.m^2.Pa)$	β $10^{-13}\,mol\,/(s.m^2.Pa^2)$	$\bar{r}$ nm
Sup	3200	233.56	258.42	539.76
Sub$_1$	35	53.5326	15.1281	137.6
Sub$_2$	35	27.497	7.4886	132.65
Sub$_2$V	80	12.4902	2.69	97.61
Sub$_2$V /Sub$_2$Vnano	-	4.5695	0.72971	77.79

Fig. 8: SEM images of Intermediate layer surface: (a) Sub$_2$, (b) Sub$_2$V and (c) Sub$_2$Vnano; and cross view:
(d) Sub$_2$, (e) Sub$_2$V and (f) Sub$_2$Vnano.
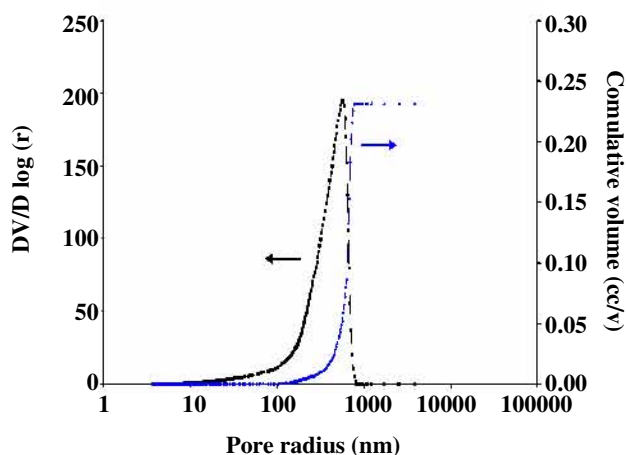
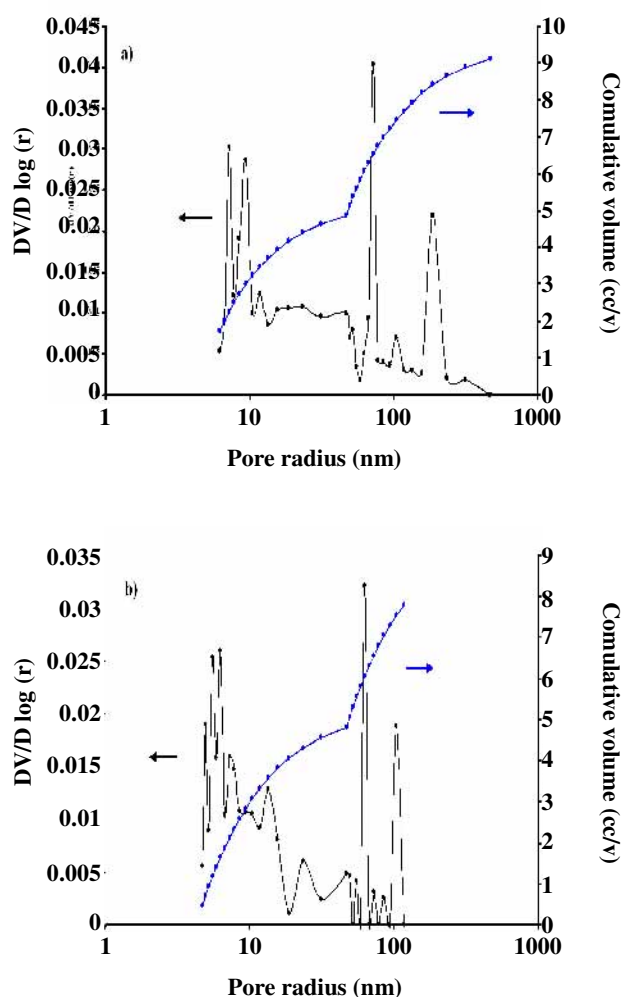*Fig. 9: Pore size distribution of untreated support (Sup.) sample.*

Fig. 10: Pore size distribution of (a) Sub₂ and (b) Sub₂Vnano samples.

alumina support versus average pressure for different modification stages. The calculated values of α_t, β_t and $\bar{r}$ for different layers of the multilayer alumina support are presented in Table 2.

For the last layer, using dilute slurry of nano particles and also applying 0.02-0.03 bar vacuum, results in partial penetration of particles through the surface pores and in spite of the considerable improvement of surface, a distinct layer could not be distinguished in cross view SEM image (Fig. 8). Hence, the two last layers were assumed as a unified layer.

Refer to Table 2, it is found that after the first modification step with submicron alumina slurry, due to the smaller particles, average pore size of surface decreases significantly (~137 nm for Sub_1). Average pore size of surface seems to be remained unchanged after the next modification step with the same solution (~133 nm for Sub_2), although the surface is improved to some extent and surface cracks are lowered. More surface modification by vacuum dip-coating of alumina submicron particles slurry results in decreasing of average pore size of the layer to 98 nm and the surface is defect free which is related to more compact of particles together in case of using the vacuum. Eventually, surface modification with alumina nano particles slurry by applying vacuum is considerable and average pore size of surface decreases to 78 nm. As presented earlier, the obtained results are in good agreement with mercury porosimetry measurements.

CONCLUSIONS

Nanostructure porous membrane supports were successfully prepared via gel-casting followed by dip-coating method. The effects of several parameters (solid content, dipping time, vacuum pressure, heating rate and number of coated layers) on the microstructure and morphology of the prepared layers were investigated and an optimum routine for this technique was presented. The obtained results showed that the optimum routine for this technique was twice coating of 5 wt% submicron slurry without applying vacuum and a dipping time of 30 s for each stage followed by vacuum dip-coating of 5wt% submicron slurry for dipping time of 15 s. To obtain a nanostructure surface with more desirable performance, another dip-coating step with 1 wt% alumina nano particles slurry at the same vacuum conditions was applied.
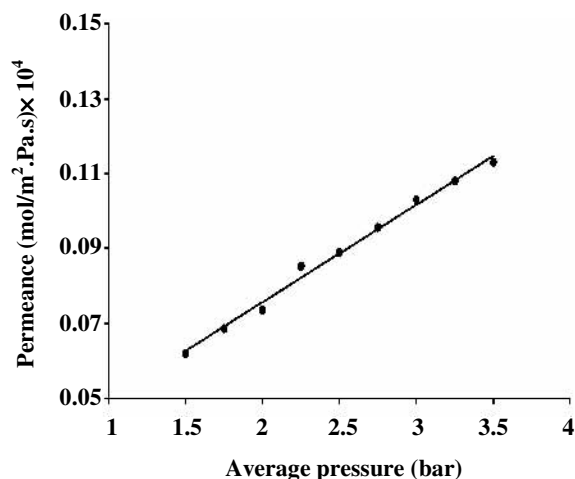
Fig. 11: Permeance of argon versus average pressure through untreated support.
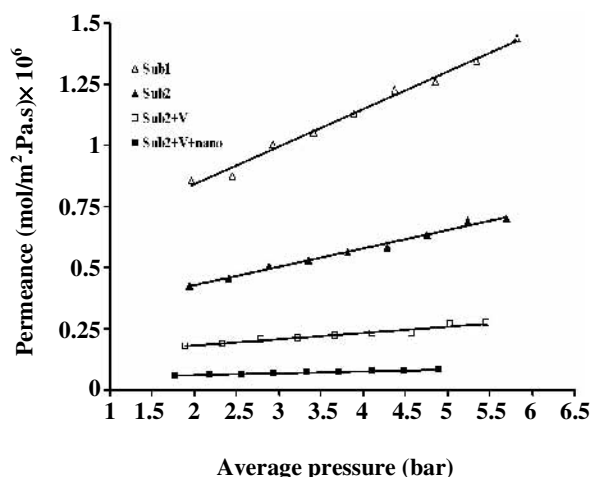

Fig. 12: Permeance of argon versus average interface pressure through a multilayer alumina support.

A low heating rate was selected for debinding stage to achieve more uniform surfaces. Single gas permeation tests were used to determine average pore size of the fabricated intermediate layers. By applying the first modification step with submicron alumina slurry, average pore size of surface decreases dramatically. Although, support surface was improved to some extent and surface cracks were lowered after next modification step, but average pore size is not affected by the second modification step. Vacuum dip-coating of the modified support in alumina submicron and nano particles slurries results in defect-free surface with significant decreasing of average pore size.

REFERENCES

[1] Agoudjil N., Benkacem T., Synthesis of Porous Ttitanium Dioxide Membranes, *Desalination*, **206**, p. 531, (2007).

[2] Masmoudi S., Larbot A., El Feki H., Ben Amar R., Elaboration and Properties of Nnew Ceramic Microfiltration Membranes from Natural and Synthesized Apatite, *Desalination*, **190**, p. 89 (2006).

[3] Yang C., Zhang G., Xu N., Shi J., Preparation and Application in Oil-Water Separation of ZrO_2/a-Al_2O_3 MF Membrane, *J. Membr. Sci.*, **142**, p. 235 (1998).

[4] Wang Y.H., Liu X.Q., Meng G.Y., Preparation and Properties of Supported 100% Titania Ceramic *Membranes, Mater. Res. Bull.*, **43**, p. 1840 (2008).

[5] Khemakhem, S., Ben Amar, R., Larbot, A., Synthesis and Characterization of a New Inorganic Ultrafiltration Membrane Composed Entirely of Tunisian Natural Illite Clay, *Desalination*, **206**, p. 210 (2007).

[6] Zhang H., Quan X., Chen S., Zhao H., Zhao Y., Li W., Zirconia and Titania Composite Membranes for Liquid Phase Separation: Preparation and Characterization, *Desalination*, **190**, p. 172 (2006).

[7] Benito J.M., Conesa A., Rubio F., Rodriguez M.A., Preparation and Characterization of Tubular Ceramic Membranes for Treatment of Oil Emulsions, *J. Eur. Ceram. So.*, **25**, p. 1895 (2005).

[8] Saffaj N. Alami Younssi S., Albizane A., Messouad, A., Bouhria M., Persin M., Cretin M., Larbot A., Preparation and Characterization of Ultrafiltration Membranes for Toxic Removal from Wastewater, *Desalination*, **168**, p. 259 (2004).

[9] Kovalevsky A.V., Kharton V.V., Snijkers F.M.M., Cooymans J.F.C., Luyten J.J., Marques F.M.B., Oxygen Transport and Stability of Asymmetric $SrFe(Al)O_{3-\delta}$-$SrAl_2O_4$ Composite Membranes, *J. Membr. Sci.*, **301**, p. 238 (2007).

[10] Ernst B., Haag S., Burgard M., Permselectivity of a Nickel/Ceramic Composite Membrane at Elevated Temperatures: A New Prospect in Hydrogen Separation, *J. Membr. Sci.*, **288**, p. 208 (2007).

[11] Gestel T.V., Vandecasteele C., Buekenhoudt A., Dotremont C., Luyten J., Leysen R., Van Der Bruggen B., Maes G., Alumina and Titania Multilayer Membranes for Nanofiltration: Preparation, Characterization and Chemical Stability, *J. Membr. Sci.*, **207**, p. 73 (2002).

[12] Burggraaf A.J., Cot L., "Fundamentals of Inorganic Membrane Science and Technology, Elsevier Science and Technology", 4th Edition, Elsevier, Amsterdam, Netherlands, (1996).

[13] Cao G.Z., Brinkman H.W., Meijerink J., de Vries K.J., Burggraaf A.J., Pore Narrowing and Formation of Ultrathin Yyttria-Stabilized Zirconia Layers in Ceramic Membranes by Chemical Vapor Deposition/ Electrochemical Vapor Deposition, *J. Am. Ceram. Soc.*, **76**, p. 2201 (1993).

[14] Lin Y.S., Burggraaf A.J., Experimental Studies on Pore size Change of Porous Ceramic Membranes After Modification, *J. Membr. Sci.*, **79**, p. 65 (1993).

[15] Lin Y.S., A Theoretical Analysis on Pore Size Change of Porous Ceramic Membranes After Modification, *J. Membr. Sci.*, **79**, p. 55 (1993).

[16] Tsai C.Y., Tama S.Y., Lu Y., Brinker C.J., Dual-Layer Asymmetric Microporous Silica Membranes, *J. Membr. Sci.*, **169**, p. 255 (2000).

[17] Babaluo A.A., Kokabi M., Manteghian M., Sarraf Mamoory M.R., A Modified Model for Alumina Membranes Formation by Gel-Casting and Dip-Coating, *J. of the European Ceramic Society*, **24**, p. 3779 (2004).

[18] Ahmadian Namini P., Babaluo A.A., Peyravi M., Akhfash M., Jannatdoust E., Synthesis of Submicron Aumina Powder via a New Wet Chemical Method, "The 5th International Chemical Engineering Congress (IChEC 2008)", 2-5 Jan, 2008, Kish Island, Iran.

[19] Tahmasebpour M., Babaluo A.A., Shafiee S., Pipelzadeh E., Studies on the Synthesis of α-Al$_2$O$_3$ Nanopowders by Polyacrylamide Gel Method, *Powder Technology*, **191**, p. 91 (2009).

[20] Anderson M. A., Gieselmann M. J., Xu Q., Titania and Alumina Membranes, *J. Membr. Sci.*, **39**, p. 243 (1988).

[21] Lin Y.S., Burggraaf A.J., Preparation and Characterization of High Temperature Thermally Stable Alumina Membrane Composite, *J. Am. Ceram. Soc.*, **74**, p. 219 (1991).

[22] Lin Y.S., Burggraaf A.J., Experimental Studies on Pore Size Change of Porous Ceramic Mmembranes After Modification, *J. Membr. Sci.*, **79**, p. 65 (1993).